

Comparison of experimental and predicted atomization characteristics of high-pressure diesel spray under various fuel and ambient temperature[†]

Su Han Park¹, Hyung Jun Kim² and Chang Sik Lee^{2,*}

¹Graduate School of Hanyang University, Department of Mechanical Engineering, Hanyang University, 17 Haengdang-dong, Sungdong-gu, 133-791, Republic of Korea

²Department of Mechanical Engineering, Hanyang University, 17 Haengdang-dong, Sungdong-gu, Seoul, 133-791, Republic of Korea

(Manuscript Received June 19, 2009; Revised February 1, 2010; Accepted April 21, 2010)

Abstract

The aim of this study is to investigate the effects of the fuel temperature and the ambient gas temperature on the overall spray characteristics. Also, based on the experimental results, a numerical study is performed at more detailed and critical conditions in a high pressure diesel spray using a computational fluid dynamics (CFD) code (AVL, FIRE ver. 2008). Spray tip penetration and spray cone angle are experimentally measured from spray images obtained using a spray visualization system composed of a high speed camera and fuel supply system. To calculate and predict the high pressure diesel spray behavior and atomization characteristics, a hybrid breakup model combining KH (Kelvin-Helmholtz) and RT (Rayleigh-Taylor) breakup theories is used. It was found that an increase in fuel temperature induces a decrease in spray tip penetration due to a reduction in the spray momentum. The increase of the ambient gas temperature causes the increase of the spray tip penetration, and the reduction of the spray cone angle. In calculation, when the ambient gas temperature increases above the boiling point, the overall SMD shows the increasing trend. Above the boiling temperature, the diesel droplets rapidly evaporate immediately after the injection from calculation results. From results and discussions, the KH-RT hybrid breakup model well describes the effects of the fuel temperature and ambient gas temperature on the overall spray characteristics, although there is a partial difference between the experimental and the calculation results of the spray tip penetration by the secondary breakup model.

Keywords: Atomization; High pressure diesel spray; Kelvin-Helmholtz and Rayleigh-Taylor hybrid breakup model; Spray tip penetration

1. Introduction

Diesel engines have many merits including high thermal efficiency, superior fuel consumption, and high power performance. By applying a common rail injection system to a diesel engine, it is possible to achieve high pressure fuel injection and control of injection timing and injection quantity for various engine speeds and loads by means of an electrical control system. However, an internal combustion engine must simultaneously reduce nitrogen oxides (NO_x), hydrocarbon (HC), carbon monoxide (CO), and particulate matter (P.M.) emissions to meet current and future emissions standards. To develop methods for meeting the increasingly stringent emission regulations, many studies are ongoing [1, 2].

Fuel spray characteristics play an important role in terms of combustion characteristics and exhaust emission formation in diesel engines in which the fuel spray is directly injected into

the combustion chamber (i.e., direct injection engines). In addition, the quality of the fuel-air mixture formation is a very important factor in reducing emissions. Therefore, spray and atomization characteristics have to be considered to optimize the design of the combustion chamber to reduce exhaust emissions and improve combustion performance. Diesel spray characteristics are influenced by the injector characteristics, injection parameters, the flow characteristics inside the combustion chamber, and whether or not the injected spray impinges upon the cylinder wall. Therefore, experimental investigations must be performed along with numerical analysis to develop an accurate method of predicting diesel spray characteristics.

Lee et al. [3] and Park et al. [4] studied the effects of the split injection on the macroscopic development characteristics of diesel spray and atomization characteristics using experimental and analytical methods in a diesel engine with a common rail injection system. They reported that the diesel spray was mainly affected by variations in ambient conditions and in the injection pressure. At the same injection pressure and mass, the spray tip penetration increased and the Sauter mean diame-

[†] This paper was recommended for publication in revised form by Associate Editor Kyoung Doug Min

*Corresponding author. Tel.: +82 2 2220 0427, Fax.: +82 2 2281 5286

E-mail address: cslee@hanyang.ac.kr

© KSME & Springer 2010

ter (SMD) increased somewhat compared to a single pilot injection. Andreassi et al. [5] experimentally and numerically studied the impingement of high pressure diesel spray and reported the effect of the injection pressure, ambient pressure, and the temperature of the impinged plate on the diesel spray behavior after the impingement. Kim et al. [6] presented atomization characteristics during the transient process of diesel spray, and reported that the SMD increased somewhat between the injection and the ligament breakup, before decreasing during ligament breakup. Besides these works, various other studies related to diesel spray and combustion are ongoing [7, 8]. However, studies that directly address the effect of the fuel temperature and ambient gas conditions on the diesel spray are insufficient within the research on diesel combustion performance and spray behavior. Therefore, a more systematic study on this topic is needed.

In this study, we explored how the various conditions including fuel temperature and state of the ambient gas affected the overall spray characteristics of diesel fuel through experimental analysis of the spray tip penetration and spray cone angle. Based on the experimental results, a numerical analysis on the spray tip penetration, atomization performance, and evaporation characteristics was conducted under the same experimental conditions. In addition, the calculated results were analyzed and compared to the experimental results by the modification of breakup model constants.

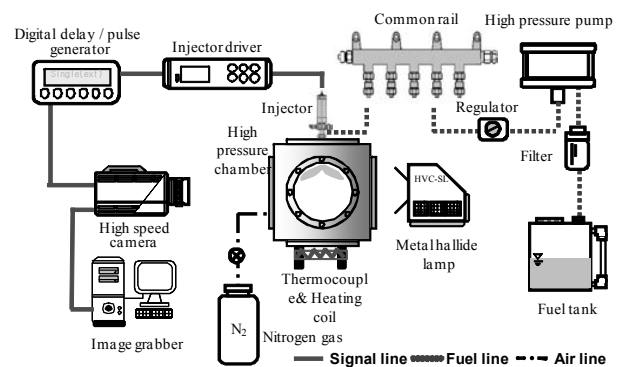
2. Experimental apparatus and procedure

A six-hole injector with nozzle hole diameters of 0.126mm was used to analyze the effects of the inlet fuel and ambient gas temperatures on the overall spray characteristics. The spray images of the fuel injected through the six holes injector were obtained from a bottom view. The detailed experimental conditions are listed in Table 1. The test injector was controlled via a solenoid signal from the injector driver (TEMS, TDA-3200H). Spray images for analyzing the spray tip penetration and spray cone angle were obtained using a high speed camera (Photron, Fastcam-APX RS) with two metal-halide lamps (Photron, HVC-SL) as light sources (Fig. 1(a)). The obtained spray images were processed on a computer using image processing software. In this work, the injection signal and the shutter signal of the high speed camera were synchronized by a digital delay/pulse generator (Berkeley Nucleonics Corp., Model 555).

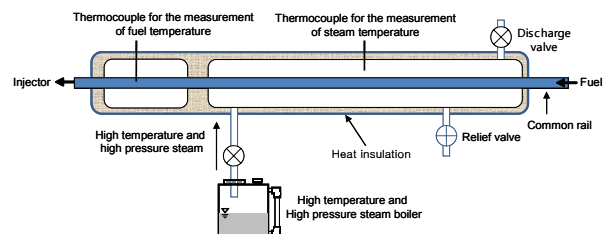
Parallel linked high pressure pumps (Haskel, HSF-300) and a common rail injection system supplied stable, high pressure diesel fuel. A heating coil and nitrogen gas were utilized in order to control the ambient gas temperature and pressure, respectively; these values were monitored with a K-type thermocouple and a pressure gauge. Fuel inlet temperature was adjusted by a fuel heating device as illustrated in Fig. 1(b). The fuel heating system consisted of a fuel supply line, a duplication tube, a high pressure-high temperature steam boiler, relief and discharge valves, and two thermocouples. The inlet

Table 1. Experimental and calculation conditions.

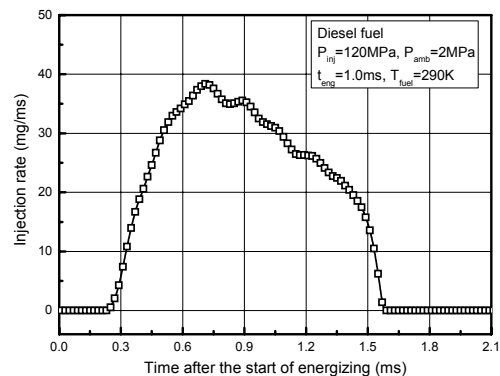
Experimental conditions	
Injection pressure (P_{inj})	120 MPa
Ambient pressure (P_{amb})	2 MPa, 4 MPa
Energizing duration (t_{eng})	1.0 ms
Fuel temperature (T_{fuel})	290K, 360K
Ambient temperature (T_{amb})	290K, 400K
Calculation conditions	
Injection pressure (P_{inj})	120 MPa
Ambient pressure (P_{amb})	2 MPa, 4 MPa
Energizing duration (t_{eng})	1.0 ms
Fuel temperature (T_{fuel})	290K, 360K, 430K, 500K
Ambient temperature (T_{amb})	290K, 400K, 600K



(a) Schematic of the spray visualization system



(b) Schematic of the fuel heating device



(c) Injection rate profile

Fig. 1. Schematic of the experimental apparatus and injection rate profile.

Table 2. Specifications of the diesel test fuel.

Fuel property	Diesel
Fuel standard	ASTM D 975
Lower Heating Value, Btu/gal	~ 129,050
Kinematic Viscosity, @ 40 °F	1.3-4.1
Specific gravity, kg/l @ 60°F	0.85
Density, lb/gal @ 15 °F	7.079
Water and sediment, vol%	0.05 max
Carbon, wt%	87
Hydrogen, wt%	13
Oxygen, by dif. wt%	0
Sulfur, wt%	0.05 max
Boiling point, °F	180 to 340
Flash point, °F	60 to 80
Cloud point, °F	-15 to 5
Pour point, °F	-35 to -15
Cetane Number	40-55
Lubricity SLBOCLE, grams	2000-5000
Lubricity HFRR, microns	300-600

Source: Biodiesel handling and use guidelines, Energy Efficiency and Renewable Energy DOE/GO-102006-2358, 3rd edition, September 2006.

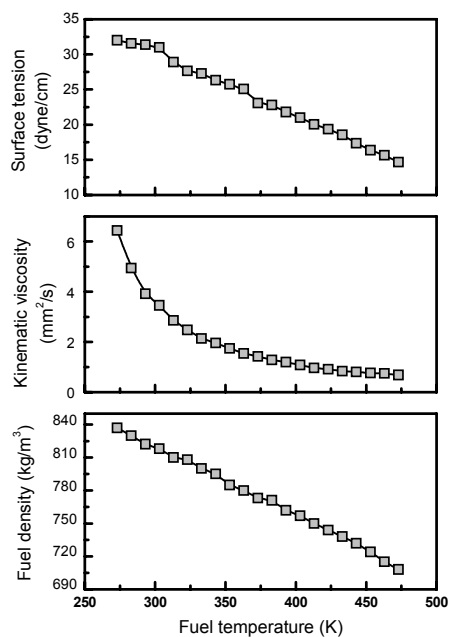


Fig. 2. Effect of the fuel temperature on the fuel properties (fuel density [9], kinematic viscosity [9]).

fuel line was wrapped with high temperature steam and the duplication tube was thereby heated to the desired temperature when the fuel was supplied to the test injector. Temperature control was achieved using the relief and discharge valves. The diesel fuel and high pressure steam temperatures were measured by two K-type thermocouples (Omega, KMTSS-020G-12) installed in the fuel line and steam line, respectively.

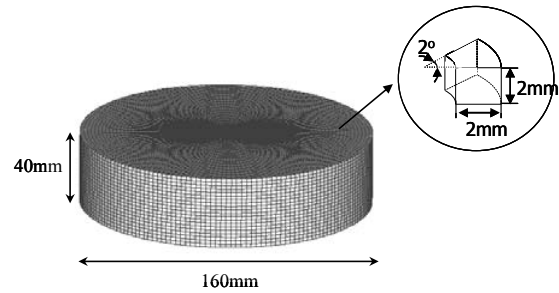


Fig. 3. Computational grid for the calculation of the diesel sprays.

In addition, Fig. 1(c) shows the injection rate profile of diesel fuel which applied to the calculation code.

In the present study, ultra low sulfur diesel (ULSD) was used as the test fuel to investigate the overall spray characteristics according to the variation of the fuel temperature and ambient gas temperature. Detailed physical properties of the ULSD are listed in Table 2. Fig. 2 shows the effects of the fuel temperature on the fuel properties of diesel fuel such as a fuel density, kinematic viscosity, and surface tension. Data related to fuel density and kinematic viscosity is cited from the paper of Yoon et al. [9], and the surface tension was measured using a surface tension meter (Itoh, 514-B2). As illustrated in Fig. 2, the fuel density and surface tension linearly decreased and the kinematic viscosity exponentially decreased with increasing temperature.

3. Numerical breakup model and the applied grid for diesel spray

3.1 Applied computational grid for the analysis of diesel spray

Fig. 3 shows the 3-D computational grid which was generated by the mesh generator in FIRE v2008 for the calculation of the diesel spray behavior. The calculation grid was of cylindrical type with a diameter of 160mm and a height of 40mm to prevent impingement onto the wall. Each individual cell of the grid was 2mm×2mm, and the total number of cell was 144,000. The calculated time interval was set to 10 μ s, and the injected rate profile obtained from the injection rate meter was applied to calculate the diesel spray performance.

3.2 Numerical analysis model

The Kelvin-Helmholtz (KH) and Rayleigh-Taylor (RT) hybrid breakup models were applied to calculate the primary and secondary droplet breakup of high pressure diesel spray, respectively. In this hybrid model, the first breakup mainly occurs by the instable growth of KH waves growing on the surface of an axisymmetric cylindrical liquid jet, and the secondary breakup occurs by the competition between the instabilities of the KH surface waves and RT disturbances. The KH instability results from the viscous force by the relative tangent motion of two different phase on the interface between liquid and gas. The breakup characteristics are determined by the maximum growth rate (Ω_{KH}) and the corresponding wave-

length (Λ_{KH}), which is calculated through curve fits of the dispersion equation suggested by Reitz [10, 11].

$$\Lambda_{KH} = 9.02r \frac{(1+0.45\text{Oh}_d^{0.5})(1+0.4\text{T}^{0.7})}{(1+0.87\text{We}_g^{1.67})^{0.6}} \quad (1)$$

$$\Omega_{KH} = \frac{(0.34+0.38\text{We}_g^{1.5})}{(1+\text{Oh}_d)(1+1.4\text{T}^{0.6})} \left[\frac{\rho R^3}{\sigma} \right]^{0.5} \quad (2)$$

From the assumption that the droplet radius (r) shrinks to r_c during the breakup time (τ_{KH}), the radius (r_n) after the time of dt can be determined. The r_c and τ_{KH} are defined as the following equations (Eq. (1) and (2)), and the r_n is determined by the proportional equation (Eq. (5)).

$$R_{KH} = C_1 \Lambda \quad (3)$$

$$\tau_{KH} = \frac{3.7C_2 R}{\Lambda_{KH} \Omega_{KH}} \quad (4)$$

$$\frac{r - r_n}{dt} = \frac{r - r_c}{\tau_{KH}} \quad (5)$$

On the other hand, RT instability can grow if the acceleration normal on the interface between the liquid and ambient gas is directed into the gas, due to the dense inertia of liquid. In case of the high pressure injection injector which is widely applied to diesel engines, the initial injection velocity of droplets is very fast, and the droplets' velocity rapidly reduces by the drag force in the engine cylinder. For this reason, the RT instability plays an important role in the droplet breakup process. The disintegration of the drop is induced by the inertia of the liquid if drops and ligaments leaving the nozzle with high velocities are strongly decelerated by the aerodynamic drag force. Dividing the drag force by the mass of the drop, the acceleration of the interface can be found,

$$a = \frac{3}{8} c_D \frac{\rho_g u_{rel}^2}{2} \quad (6)$$

where c_D is the drag coefficient of the drop. Using a linear stability analysis [12] and neglecting liquid viscosity [13], the growth rate (Ω_{RT}), the corresponding wavelength (Λ_{RT}), and the wave number (K_{RT}) of the fastest growing wave is [14-16]:

$$\Omega_{RT} = \sqrt{\frac{2}{3\sqrt{3}} \frac{g_l |(\rho_d - \rho_c)|^{1.5}}{\rho_d + \rho_c}} \quad (7)$$

$$K_{RT} = \sqrt{\frac{g_l |\rho_d - \rho_c|}{3\sigma}} \quad (8)$$

$$\Lambda_{RT} = C_4 \frac{\pi}{K_{RT}} \quad (9)$$

The RT breakup time (τ_{RT}) and the droplet radius (r_c) after breakup are as follows.

$$\tau_{RT} = C_5 \frac{1}{\Omega_{RT}} \quad (10)$$

$$r_c = \frac{\pi C_{RT}}{K_{RT}} \quad (11)$$

Therefore, the droplet breakup by the KH-RT hybrid breakup model is progressing as the following algorithm. If the droplet breakup calculation starts, the calculated RT wavelength is compared to the droplet diameter. If the RT wavelength is smaller than the droplet diameter, it is assumed that the RT wave grows on the droplet surface. When the growth of waves is predicted on the droplet surface, the growth period of waves is calculated and compared to breakup time obtained from Eq. (10). If the wave growth is longer than the breakup time, it is assumed that droplet breakup occurs by the RT breakup model. In addition, it is assumed that the droplet breakup is not occurring if the inertial force of droplets is smaller than the surface tension force. The change of the droplet velocity is calculated from the assumption that the total energy (kinetic energy + surface energy) after breakup is the same with that before breakup.

Heat and mass transfer processes between droplets and the ambient are described by a model originally derived by Dukowicz [17]. This model is based on the following assumptions: spherical symmetry, quasi gas-film around the droplet, uniform droplet temperature along the drop diameter, uniform physical properties of the surrounding fluid, and liquid-vapor thermal equilibrium on the droplet surface. Under the assumption of uniform droplet temperature, the rate of droplet temperature change is determined by the energy balance equation, which states that the energy conducted to the droplet either increases the temperature of the droplet or supplies heat for vaporization.

$$m_d c_{pd} \frac{dT_d}{dt} = L \frac{dm_d}{dt} + \dot{Q} \quad (12)$$

The convective heat flux \dot{Q} supplied from the gas to the droplet surface is $\dot{Q} = \alpha A_s (T_\infty - T_s)$, where α is the convective heat transfer coefficient through the film surrounding the droplet in the absence of mass transfer, and A_s is the droplet surface area.

Turbulent dispersion of the spray was described by the models suggested by O'Rourke [18]. This approach sets the fluctuating components to zero but calculates a new particle location and velocity, instead of reducing the spray integration time step. For each component the velocity and position distribution are Gaussian. In addition, a model of droplet interaction by O'Rourke and Bracco [19], which accounts for coalescence and collision, was applied to the calculation code.

4. Results and discussion

4.1 Effects of the fuel temperature on the overall spray characteristics

The experimental and numerical spray images for variations in diesel fuel temperature are represented in Fig. 4. The color bar index indicates the droplet velocity. Externally, the spray

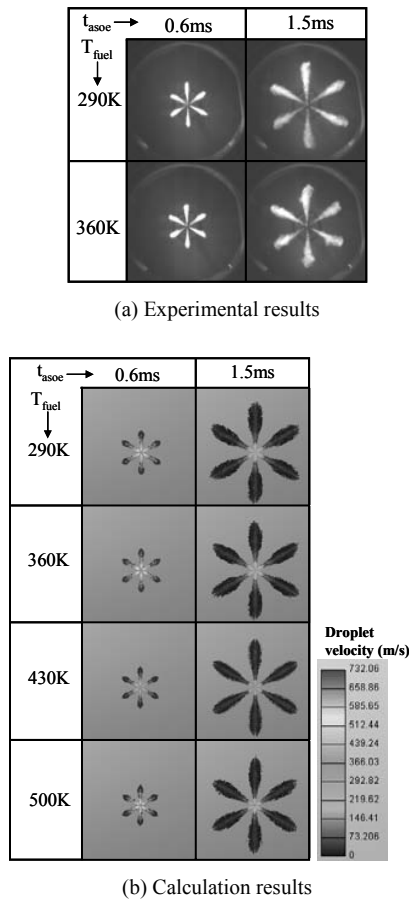


Fig. 4. Comparison between the experimental and calculation results according to the variation of the diesel fuel temperature ($P_{inj}=120$ MPa, $P_{amb}=4$ MPa, $t_{eng}=1.0$ ms).

images of Fig. 4(a) and Fig. 4(b) have a similar spray shape and developing pattern. Also, the calculated droplet velocity distribution showed a similar trend for all fuel temperature cases. The velocity shows the highest value near the nozzle tip, and it shows a low value at a faraway distance from the spray core. This is the reason why the mass and momentum transfer between the droplets and ambient gas are actively occurring. The experimental spray images were well described by the calculated spray images. From the experimental and numerical results, it seems that the macroscopic spray characteristics were such as the spray developing pattern and spray shape hardly affected by fuel temperature. A quantitative analysis of spray characteristics is shown in detail in Fig. 5 and Fig. 6.

Fig. 5 shows the quantitative spray characteristics such as the spray tip penetration and spray cone angle in various fuel temperature conditions through the analysis of the spray images. Especially, the comparison between the experimental and numerical spray tip penetration is illustrated in Fig. 5(a). The error bar included in the figure represents the experimental error range. Test conditions were an injection pressure of 120 MPa, an ambient gas pressure of 4 MPa, and a 1.0ms of an energizing duration. Spray tip penetration is defined as the maximum distance between the injected spray end and the

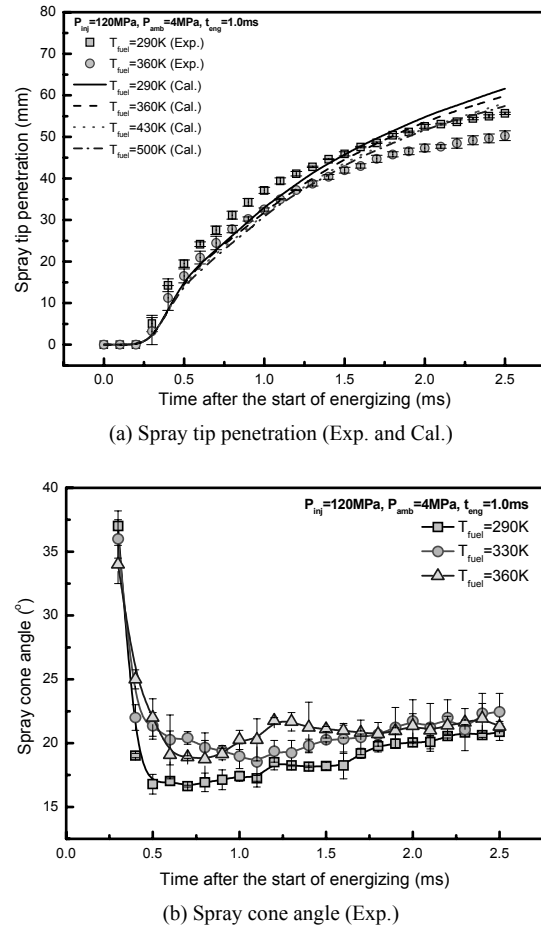


Fig. 5. Effect of the fuel temperature on the spray tip penetration and spray cone angle ($P_{inj}=120$ MPa, $P_{amb}=4$ MPa, $t_{eng}=1.0$ ms).

nozzle tip when the diesel spray is injected into the stagnant gas in the high pressure chamber. The spray cone angle is defined as the angle between the two lines formed by the nozzle tip and two maximum radial distance points. As illustrated in Fig. 5(a), the experimental spray tip penetration decreased with the increase of the fuel temperature, because the increase of the fuel temperature induces the reduction of density, and it results in a decrease in the spray momentum. In the calculation results, the spray tip penetration also decreased with the increase of the fuel temperature. In both experimental and calculation results, the reduction level of the spray tip penetration became large with elapsed time after the start of energizing. It is the reason why the spray behavior during the energizing is affected by the injection pressure and initial spray momentum, while the spray tip penetration is mainly affected by the ambient gas conditions after the end of energizing [20]. Therefore, spray tip penetration decelerated because high fuel temperature diesel spray has a low kinematic viscosity and a low surface tension; therefore, the spray momentum of droplets was quickly lost. On the other hand, the spray cone angle increases when fuel temperature increases. This result shows that the spray cone angle is inversely proportional to the fuel density [21]. It can be postulated that the spray momentum

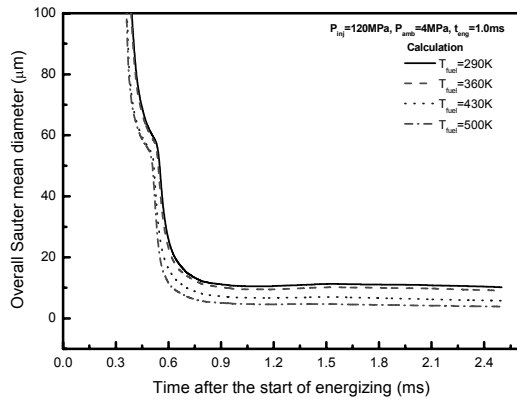


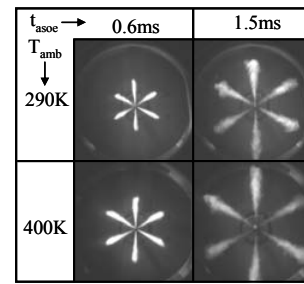
Fig. 6. Calculated overall SMD distribution at various fuel temperature ($P_{inj}=120$ MPa, $P_{amb}=4$ MPa, $t_{eng}=1.0$ ms).

largely resulted in a decrease in spray momentum in the axial direction compared to the radial spray momentum. In addition, the spray cone angle suddenly decreased after the injection due to a rapid increase in axial spray distance, and then subsequently gradually increased or converged.

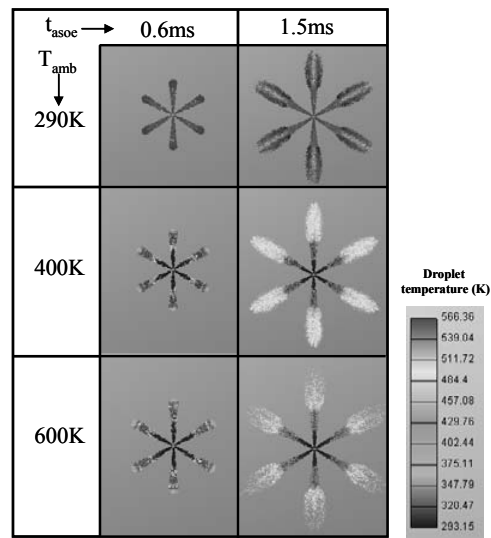
Fig. 6 shows the overall Sauter mean diameter (SMD) distribution at various fuel temperatures. The fuel temperature of diesel varied from 290K to 500K as an interval of 70K. The overall SMD is indicative of the time-dependent average droplet size at a specific time when evaluating the group of droplets as whole. The droplet diameter suddenly decreased immediately after injection due to a fast velocity at the nozzle exit, where it reached a uniform value. The increased fuel temperature induced a decrease in the overall SMD, because considering the boiling point of diesel fuel, the increased fuel temperature induces the change of the fuel properties such as the decrease of the kinematic viscosity and the surface tension, and simultaneously it causes an active droplet breakup.

4.2 Effects of the ambient gas conditions on the overall spray characteristics

Fig. 7 shows a comparison between the experimental and calculated results according to a variation of the ambient gas temperature for the following test conditions: 120 MPa injection pressure, 2 MPa ambient gas pressure, 1.0 ms energizing duration, and 290K diesel fuel temperature. The color index on the right side of Fig. 7(b) indicates the droplet temperature. The experimental spray images are well described by the calculated results. In addition, it can be seen that the spray development is more active at high ambient gas temperatures. In terms of the calculated results, the droplet temperature of the injected diesel spray increased with the ambient gas temperature, and the increasing droplet temperature affected the droplet properties [9]. From this result, it is expected that the atomization and evaporation characteristics were changed due to the change in droplet properties. At 1.5ms of the time after the energizing, the droplet concentration of the injected spray is low. It is believed the high ambient gas temperature induces active droplet evaporation. The quantitative effects of the am-



(a) Experimental results

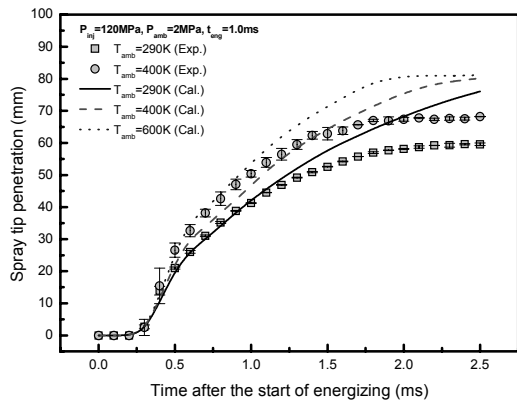


(b) Calculation results

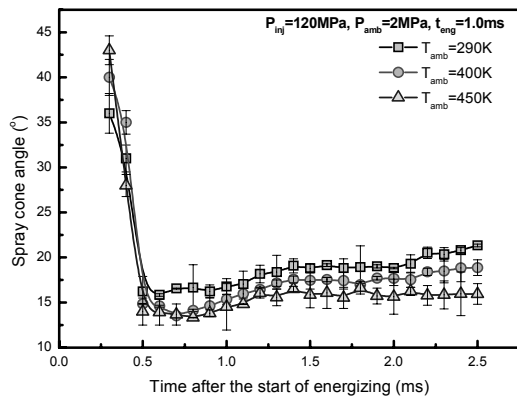
Fig. 7. Comparison between the experimental and calculation results according to the variation of the ambient gas temperature ($P_{inj}=120$ MPa, $P_{amb}=2$ MPa, $t_{eng}=1.0$ ms, $T_{fuel}=290$ K).

bient gas temperature on the atomization and evaporation characteristics are minutely explained in Fig. 8 and Fig. 9.

The comparison between the experimental and numerical results of spray tip penetration for the variation of the ambient gas temperatures is shown in Fig. 8(a). The numerical analysis method predicted the trends of the experimental results for the effect of the ambient gas temperature on the spray tip penetration quite well. An increase in the ambient gas temperature causes a decrease in the ambient gas density according to the ideal gas law. Low ambient gas density leads to the active development of the spray tip penetration. As illustrated in Fig. 8(a), the spray tip penetration increased with the increase of the ambient gas temperature, and it can be also confirmed the same tendency in the calculation results. At an ambient gas temperature of 290K, the gap between the experimental and numerical results became large from 1.3 ms after the start of energizing. This is the reason why the droplets after the end of injection start the quick momentum loss by the aerodynamic drag force in experiments. However, it is believed that in the calculation process, the various factors which are influencing the spray characteristics in the RT model for the secondary breakup are not perfectly reflecting the change of the ambient



(a) Spray tip penetration

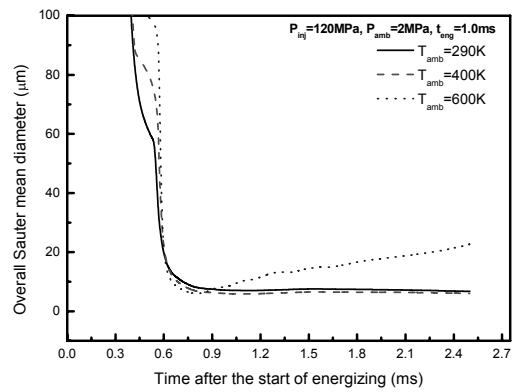


(b) Spray cone angle

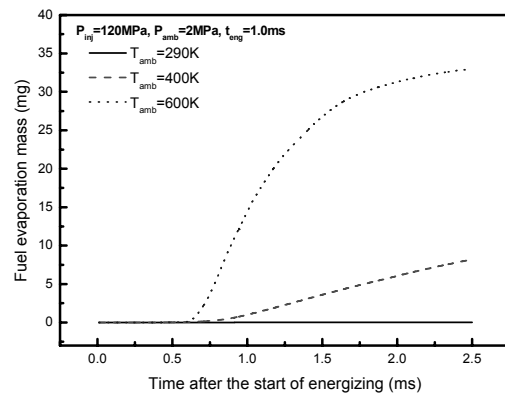
Fig. 8. Effect of the ambient gas temperature on the spray tip penetration and spray cone angle ($P_{inj}=120$ MPa, $P_{amb}=2$ MPa, $t_{eng}=1.0$ ms).

gas temperature. Fig. 8(b) shows how the variation of the ambient gas temperature affects the behavior of the spray cone angle. The spray cone angle gradually decreased with increasing ambient gas temperature. This is the reason why the small droplets in the outer region of the injected spray quickly evaporated, and the spray cone angle had a tendency to be proportional to the ambient gas density.

Fig. 9 shows the calculated overall SMD and the fuel evaporation mass at three ambient gas temperatures. The ambient gas pressure and energizing duration are 2 MPa and 1.0ms, respectively. As illustrated in Fig. 9(a), when the ambient gas temperature increases from 290K to 400K, the overall SMD shows little difference, and it starts to decrease lately. This is because at conditions below the boiling temperature (around 580K~700K), the diesel droplets experience much breakup and little evaporation on the droplet surface. However, at a condition above the boiling temperature, diesel droplets quickly evaporated, leaving only the large droplets remaining in the calculation region. Therefore, it is believed that this phenomenon and coalescence among droplets results in the increase of the overall SMD at 600K of the ambient gas temperature. In the ambient gas temperature conditions of below and above the boiling temperature, the evaporation character-



(a) Overall SMD distribution



(b) Fuel evaporation mass

Fig. 9. Calculated overall Sauter mean diameter and fuel evaporation characteristics at various ambient gas temperature ($P_{inj}=120$ MPa, $P_{amb}=2$ MPa, $t_{eng}=1.0$ ms).

istics of diesel droplets are shown in Fig. 9(b). As shown in Fig. 9(b), the diesel fuel quickly evaporated after the end of the injection ($t_{eng}=1.0$ ms) at 600K, compared to the other cases. In addition, the fuel evaporated mass increased when the injected fuel droplets approached the diesel boiling point. It is believed that these evaporation characteristics of diesel fuel affect the atomization characteristics as illustrated in Fig. 9(a).

5. Conclusions

An experimental and analytical investigation on the overall spray characteristics of diesel fuel was conducted at various fuel temperatures and ambient gas conditions. Based on the experimental results, a numerical study was performed at more detailed conditions. From the results and discussion in this paper, the conclusions are summarized as follows.

(1) The increase of the fuel temperature induced a decrease of the spray tip penetration due to the reduction of the spray momentum by the decrease of the fuel density, while the spray cone angle showed an increasing trend in the experiments and calculations. The numerical analysis using KH-RT hybrid breakup model well predicted the experimental spray patterns

according to the variation of the fuel temperature.

(2) The calculated droplet size decreases by the increase of the fuel temperature due to the decrease of the kinematic viscosity and surface tension. Another reason is that the increased fuel temperature induces the short breakup length and active droplet breakup.

(3) The increase of the ambient gas temperature causes the increase of the spray tip penetration, and the reduction of the spray cone angle. In calculation, when the ambient gas temperature increases above the boiling point, the overall SMD shows the increasing trend. This is due to the quick evaporation of diesel droplets and the remains of the large droplets in the calculation region. Above the boiling temperature, the diesel droplets rapidly evaporate immediately after the injection from calculation results.

(4) The KH-RT hybrid breakup model well describes the effects of the fuel temperature and ambient gas temperature on the overall spray characteristics, although there is a partial difference between the experimental and the calculation results of the spray tip penetration by the secondary breakup model.

Acknowledgment

This work was supported in part by the CEFV (Center for Environmentally Friendly Vehicle) of the Eco-STAR project of the MOE (Ministry of the Environment in Seoul, Republic of Korea) and the Second Brain Korea 21 Project in 2009. This work was financially also supported by a manpower development program for Energy & Resources supported by the ministry of knowledge and economy (MKE).

Nomenclature

A_s	: Particle surface area (m^2)
C_1, C_2, C_3, C_4, C_5	: Breakup constants according to atomization model
C_{pd}	: Specific heat of a liquid droplet (J/kg K)
g	: Deceleration coefficient
L	: Breakup length (m)
m_d	: Particle mass (kg)
Oh_d	: Ohnesorge number for the droplets
P_{amb}, P_{inj}	: Ambient pressure, injection pressure (MPa)
\dot{Q}	: Convective heat flux (W)
R	: Droplet radius (m)
T	: Taylor number ($= Oh_d We^{1/2}$)
T_d, T_s, T_∞	: Droplet, droplet surface, particle far-field temperature (K)
T_{amb}, T_{fuel}	: Ambient gas temperature, fuel temperature (K)
We_g	: Weber number for the ambient gas
ρ	: Density (kg/m^3)
σ	: Surface tension (dyne/cm)
τ	: Breakup time (s)
λ	: Wavelength of fastest growing wave (m)
Ω	: Growth rate of most unstable wave (s^{-1})

References

- [1] D. S. Kim, M. Y. Kim and C. S. Lee, Combustion and emission characteristics of a partial homogeneous charge compression ignition engine when using two-stage injection, *Combustion Science and Technology*, 179 (2007) 531-551.
- [2] D. Kim, I. Ekoto, W. F. Colban and P. C. Miles, In-cylinder CO and UHC imaging in a light-duty diesel engine during PPCI low-temperature combustion, *SAE technical paper*, SAE 2008-01-1602.
- [3] C. S. Lee, K. H. Lee, R. D. Reitz and S. W. Park, Effect of split injection on the macroscopic development and atomization characteristics of a diesel spray injected through a common-rail system, *Atomization and Sprays*, 16 (2006) 543-562.
- [4] S. W. Park, H. K. Suh and C. S. Lee, Effect of a split injection on spray characteristics for a common-rail type diesel injection system, *International Journal of Automotive Technology*, 6 (2005) 315-322.
- [5] L. Andreassi, S. Ubertini and L. Allocca, Experimental and numerical analysis of high pressure diesel spray-wall interaction, *International Journal of Multiphase Flow*, 33 (2007) 742-765.
- [6] D. J. Kim and J. K. Lee, Analysis of the transient atomization characteristics of diesel spray using time-resolved PDPA data, *International Journal of Automotive Technology*, 9 (2008) 297-305.
- [7] S. W. Park and R. D. Reitz, Numerical study on the low emission window of homogeneous charge compression ignition diesel combustion, *Combustion Science and Technology*, 179 (2007) 2279-2307.
- [8] L. M. Ricart, R. D. Reitz and J. E. Dec, Comparison of diesel spray liquid penetration and vapor fuel distribution with in-cylinder optical measurements, *Journal of Engineering for gas turbines and power*, 122 (2000) 588-595.
- [9] S. H. Yoon, S. H. Park and C. S. Lee, Experimental investigation on the fuel properties of biodiesel and its blends at various temperature, *Energy & Fuels*, 22 (2008) 652-656.
- [10] R. D. Reitz, Modeling atomization processes in high-pressure vaporizing sprays, *Atomization and spray technology* 3, (1987) 309-337.
- [11] R. D. Reitz and F. V. Bracco, Mechanism of breakup of round liquid jets, *In Encyclopedia of Fluid Mechanics*, Gulf Pub, NJ, 3, 233-249.
- [12] S. K. Chang, Hydrodynamics in liquid jet sprays, Ph. D Thesis, University of Wisconsin-Madison, 1991.
- [13] R. Bellman and R. H. Pennington, Effects of surface tension and viscosity on Taylor instability, *Quarterly of Applied Mathematics*, 12 (1954) 151-162.
- [14] T. F. Su, M. Patterson and R. D. Reitz, Experimental and numerical studies of high pressure multiple injection sprays, *SAE technical paper*, SAE 960861 (1996).
- [15] M. A. Patterson and R. D. Reitz, Modelling the effect of fuel spray characteristics on diesel engine combustion and emission, *SAE technical paper*, SAE 980131 (1998).
- [16] M. Chan, S. Das and R. D. Reitz, Modeling multiple injection and EGR effects on diesel engine emissions, *SAE tech-*

nical paper, SAE 972864 (1997).

- [17] J. K. Dukowics, Quasi-steady droplet change in the presence of convection, *informal report Los Alamos Scientific Laboratory*, LA7997-MS.
- [18] P. J. O'Rourke, Statistical properties and numerical implementation of a model for droplet dispersion in turbulent gas, *Journal of Computational Physics*, 83 (1989).
- [19] P. J. O'Rourke and F. V. Bracco, Modelling of drop interaction in thick sprays and a comparison with experiments, *Journal of Automobile Engineering* (1980).
- [20] I. V. Roisman, L. Araneo and C. Tropea, Effect of ambient pressure on penetration of a diesel spray, *International Journal of Multiphase Flow* 33 (2007) 904-920.
- [21] H. Hiroyasu and M. Arai, Structures of fuel sprays in diesel engines, *SAE technical paper* (1990) SAE900475.



Su Han Park received his B. S and M. S. degrees from the department of Mechanical Engineering, Hanyang University in 2006 and 2008, respectively. He is currently a Ph. D. candidate. His research interests are the exhaust emission reduction related to spray-atomization characteristics of alternative fuels (biodiesel,

DME, bioethanol etc.)



Hyung Jun Kim received Ph. D degree from Hanyang University in 2010. Also, he received B. S. and M. S. degrees from Hanyang University in 2001 and 2003, respectively. Dr. Kim is currently a Post Doctorate at BK21 innovation design working group in Hanyang University. His research interests are on

spray and combustion analysis using KIVA-3V as numerical method.



Chang Sik Lee received the Ph. D degree from Hanyang University in 1980. Also, he received B. S. and M. S. degrees from Hanyang University in 1967 and 1974, respectively. Dr. Lee is currently a professor at the Department of Mechanical Engineering in Hanyang University, Seoul, Korea. His research interests are

on the development of the alternative fueled vehicle and the improvement of the combustion and emission characteristics in the internal combustion engine.